TIR RXI collimator

Dejan Grabovičkić,[1,*] Pablo Benítez,[1,2] and Juan C. Miñano[1,2]

[1]*CEDINT, Universidad Politécnica de Madrid (UPM), Campus de Montegancedo 28223 Pozuelo, Madrid, Spain*
[2]*LPI 2400 Lincoln Ave., Altadena, California 91001, USA*
**dejan@cedint.upm.es*

Abstract: A metal-less RXI collimator has been designed using the Simultaneous multiple surface method (SMS). Unlike conventional RXI collimators, whose back surface and parts of the front surface have to be metalized, this collimator is completely metal-free, made only of plastic (PMMA). The collimator's back surface is designed as a grooved surface providing two TIR reflections for all rays impinging on it. One advantage of the design is the lower manufacturing cost, since there is no need for the expensive process of metalization. More importantly, unlike conventional RXI collimators, this design performs good colour mixing, as well as being very insensitive to the source non-uniformities. The experimental measurements of the first prototype show good agreement with the simulated design.

OCIS codes: (080.2740) Geometric optical design; (080.4298) Nonimaging optics.

References and links

1. J. C. Miñano, J. C. Gonźlez, and P. Benítez, "RXI: a high-gain, compact, nonimaging concentrator," Appl. Opt. **34**(34), 7850–7856 (1995).
2. F. Muñoz, *Sistemas ópticos avanzados de gran compactibilidad con aplicaciones en formación de imagen y en iluminación*, (Thesis Doctoral, E.T.S.I.Telecomunicación, Madrid, 2004)
3. F. Muñoz, P. Benítez, O. Dross, J. C. Miñano, and B. Parkyn, "Simultaneous multiple surface design of compact air-gap collimators for light-emitting diodes," Opt. Eng. **43**(7), 1522–1530 (2004).
4. R. Winston, J. C. Miñano, and P. Benítez, with contributions of N. Shatz and J. Bortz, *Nonimaging Optics*, (Elsevier, Academic Press, 2004)
5. D. Grabovičkić, P. Benítez, and J. C. Miñano, "Free-form V-groove reflector design with the SMS method in three dimensions," Opt. Express **19**(S4 Suppl 4), A747–A756 (2011).
6. Synopsys software package LightTools, http://www.opticalres.com/
7. P. Benítez, J. C. Miñano, and A. Santamaría, "Analysis of microstructured surfaces in two dimensions," Opt. Express **14**(19), 8561–8567 (2006).
8. P. Benítez, J. C. Miñano, A. Santamaría, and M. Hernández, "On the analysis of rotational symmetric microstructured surfaces," Opt. Express **15**(5), 2219–2233 (2007).

1. Introduction

An RXI collimator is a device made up of two optical surfaces: a front surface and a back surface; Fig. 1(a). The collimator's name comes from the description of the ray trajectories. A ray coming from the source is reflected first by the TIR on the front surface (I), it is then reflected specularly onto the mirrored back surface (X) and it finally leaves the collimator after being refracted on the front surface (R). There is a small central region on the front surface that has to be metalized as well, since the TIR conditions are not satisfied for the rays impinging on this surface for the first time [1]. The LED and the collimator must be joined together with silicon to avoid the influence of the air gap. This complicates the manufacturing process, so another improved design was proposed by Muñoz and Benítez [2,3], Fig. 1(b). This collimator contains an additional surface that separates the LED from the optics. Along the ray path there is another refraction (on the entrance surface), so this collimator is called RIXR. The back surface and the central part of the front surface are metalized as in the first RXI design.

#154985 - $15.00 USD Received 19 Sep 2011; revised 8 Nov 2011; accepted 18 Nov 2011; published 6 Dec 2011

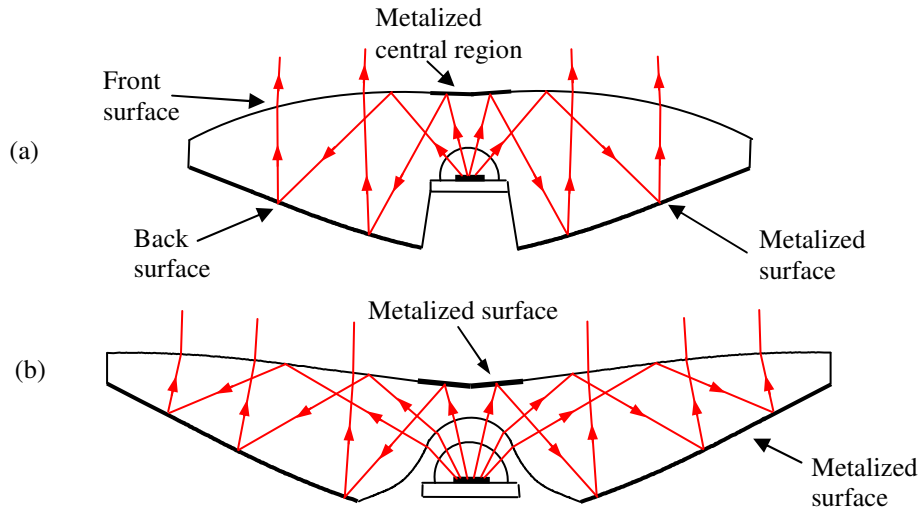

Fig. 1. Existing designs (a) RXI collimator, (b) RIXR collimator.

2. TIR RXI collimator

Here, we present a metal-less TIR collimator. This collimator is designed like a conventional RIXR, whose metalized back surface is replaced by a properly calculated grooved surface. In our design, a ray coming from a light source refracts first on the entrance surface, then reflects at onto the front surface by the TIR, and reaches the back surface. On the back surface the ray is reflected twice by the TIR at each groove side and redirected toward the front surface, where the ray will be refracted again (Fig. 2).

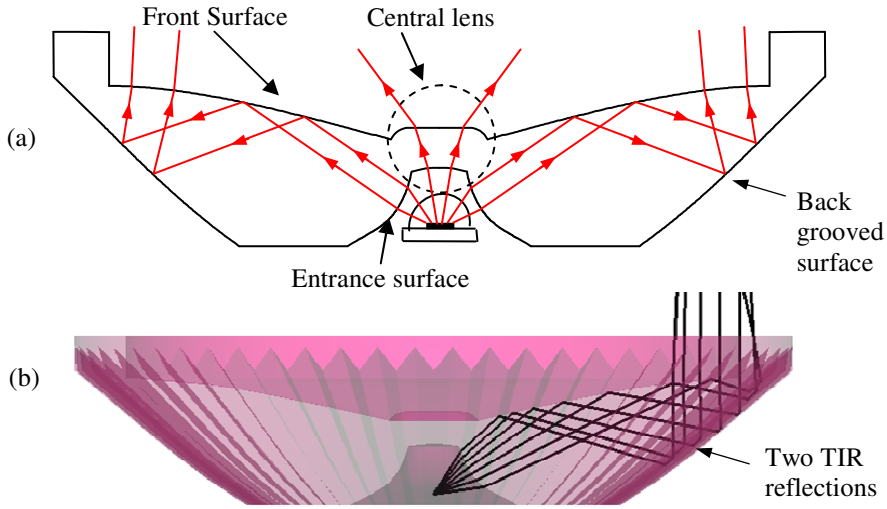

Fig. 2. Metal-less TIR RXI (a) Cross section (b) 3D View with the rays traced in LightTools.

The central part of the front surface can be replaced by a grooved surface as well. However, since this surface is close to the optical axis, the grooves are very small. This complicates the manufacturing process, so we decided to replace the central part with a lens. This lens provides a smooth intensity pattern for background illumination (from 10°-30°, as

#154985 - $15.00 USD Received 19 Sep 2011; revised 8 Nov 2011; accepted 18 Nov 2011; published 6 Dec 2011

shown in Fig. 8), which is of interest in applications such as flashlights and head-mounted lights.

3. Design procedure

3.1 2D design

In 2D we calculate our TIR RXI as an RIXR design, using the procedure explained in [2]. The design procedure starts by defining the first segments of the front surface A_0A_2 (which can be done freely), the back surface B_0B_1 (Cartesian Oval coupling the rays from A_2 and virtual source Q) and the entrance surface C_0C_1 (Cartesian Oval coupling the rays from L_- and A_2), as shown in Fig. 3. Next, we need to check the TIR conditions at point A2. If they are not satisfied, we prescribe a different form of segment A_0A_2. The rest of the entrance surface (C_1C_n) can be chosen freely [2]. For the ease of manufacture we have chosen an arc of a circumference having the same derivative as the segment C_0C_1 at C_1.

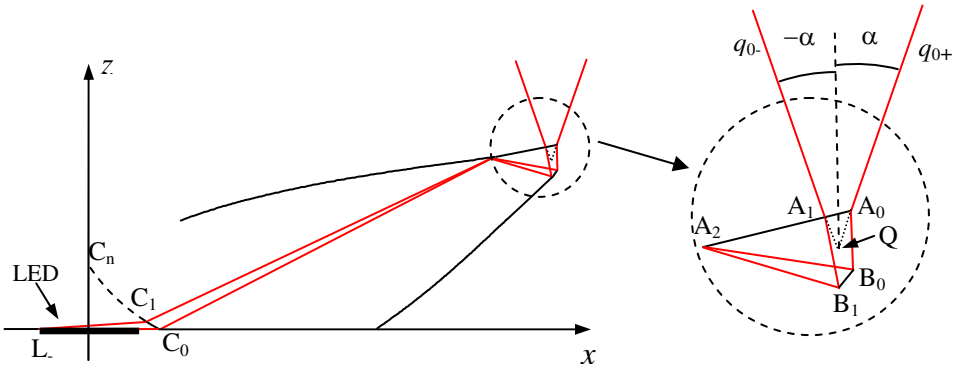

Fig. 3. 2D design procedure. Initial conditions.

Since the entrance surface is completely defined, we are able to calculate the other two surfaces using the Simultaneous Multiple Surface Design method in two dimensions (SMS2D) [4]. Consider the set of parallel rays, contained between q_{0+} and q_{x+} (Fig. 4, the rays in red). If we refract them on the front surface, then reflect them on the previously calculated segment B_0B_1, we are able to find a new piece of the front surface A_2A_3 as a free-form surface that couples the rays coming from B_0B_1 and L_-. Now, we trace the rays from another LED extreme point L_+ (Fig. 4, the rays in blue). These rays are reflected at the previously calculated segment A_2A_3 and then coupled with the set of parallel rays contained between q_{0-} and q_y. As a result, a new piece of the back surface B_1B_2 is obtained. The procedure continues thereafter repeating the last two steps alternately (shown in Fig. 4) to build both surfaces entirely.

#154985 - $15.00 USD Received 19 Sep 2011; revised 8 Nov 2011; accepted 18 Nov 2011; published 6 Dec 2011

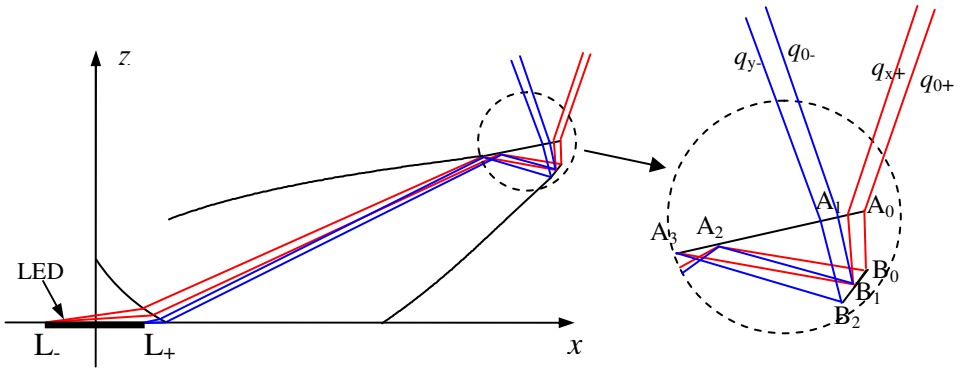

Fig. 4. Calculation of the 2D design using the SMS method.

Note that during the procedure each reflection has to be checked at the front surface. If the TIR conditions are not satisfied, the procedure stops.

3. 2 3D TIR RXI design

Once the 2D model is designed, we replace the mirrored back surface with a properly-calculated grooved reflector. Since, the entrance and the front surface are known, we are able to calculate the wavefronts impinging on the mirrored surface and reflecting from it. We have named them WF_A and WF_B. Then, the collimator's back surface (Fig. 5) can be constructed as a grooved surface using the procedure explained in [5]. The V-grooved surface provides a coupling between the two wavefronts after two TIR reflections at the V-groove, no matter which side of the groove the rays hit first.

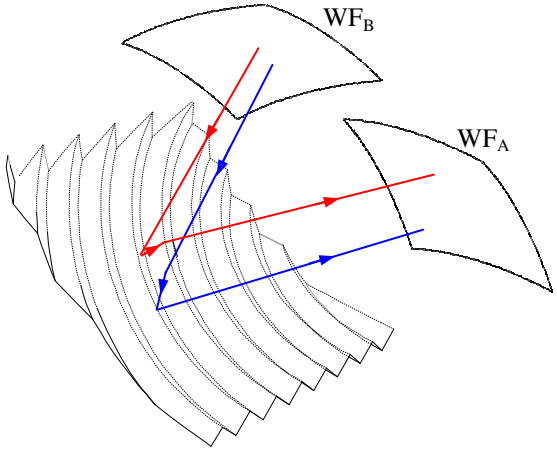

Fig. 5. Grooved surface substitute for the RIXR back surface.

In general, each groove comprises two free-form surfaces joined together along the groove edge-line (Fig. 6(a)). However, for the ease of manufacture, we decided to approximate the design using the flat V-grooves. A flat groove has a free-form edge-line, but its cross section (the plane perpendicular to the edge-line) is merely a 90° corner (the line in red, Fig. 6(b)). Since the V-groove sides are mutually perpendicular at the groove edge-line [5], this

#154985 - $15.00 USD Received 19 Sep 2011; revised 8 Nov 2011; accepted 18 Nov 2011; published 6 Dec 2011

approximation is very good as long as the grooves are small. In our case, the groove-edge line coincides with the curve that defines back surface in the 2D RIXR model.

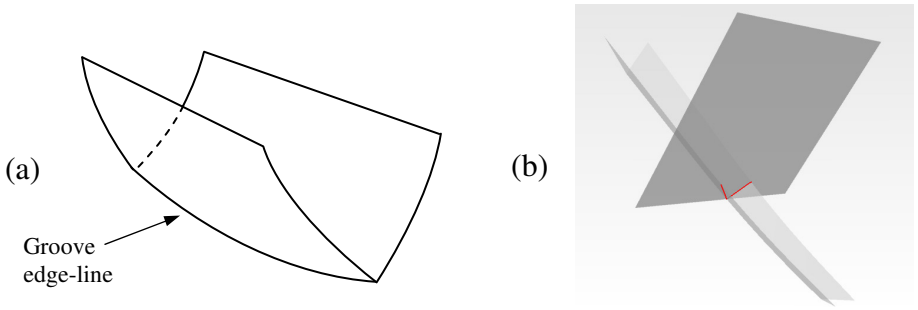

Fig. 6. (a) Free-form groove, (b) Flat V-groove. The cross section is a 90° corner (the line in red).

The number of the V-grooves can be chosen freely. The larger the number, the smaller the grooves. Resulting from the restrictions on the size of the grooves given by the manufacturer, we have designed model with 60 equal flat V-grooves (Fig. 7). The size of the groove's cross section changes along the curved edge-line, from c = 0.6 mm to c = 1.15 mm, c being the longitud of each corner side. Figure 7 shows the final TIR RXI design, the one that has been chosen for the protype. This model has been manufactured and characterized.

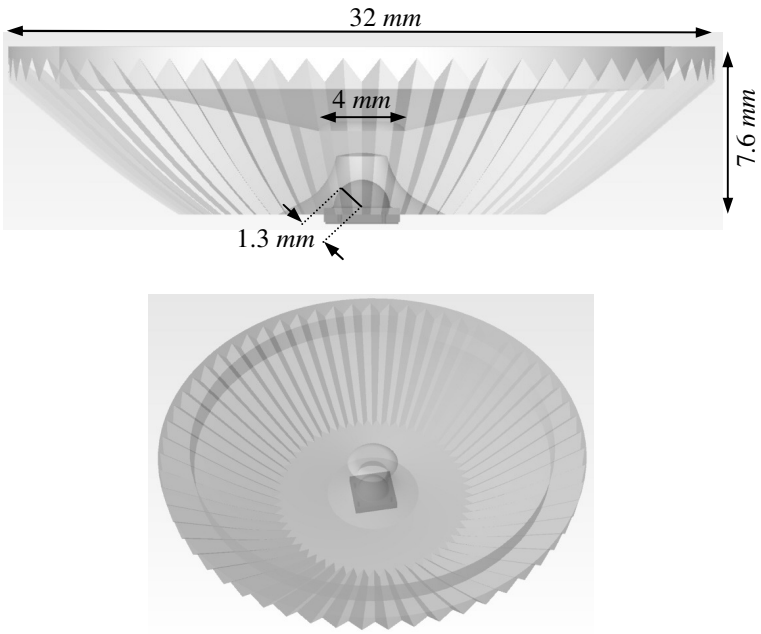

Fig. 7. TIR RXI model for manufacture with XP-G Cree LED.

3.3 Simulations of the design

The TIR RXI prototype is simulated in LightTools [6]. The LED has been modeled using the ray set of an XP-G Cree white LED (this ray set is provided by the manufacturer). Figure 8 shows the simulated far field pattern (LED power is 1*lm*). Most of the power has reached the far field receiver within the 10° x 10° square (about 69.1%), about 88.6% of the power arrives

#154985 - $15.00 USD Received 19 Sep 2011; revised 8 Nov 2011; accepted 18 Nov 2011; published 6 Dec 2011

within the 30° x 30° square. The smooth part of the intensity pattern (from 10°-30°) is obtained through a proper design of the central lens. The full-width half-maximum angle is 4.5° and the maximum value of the simulated intensity is 28cd/lm.

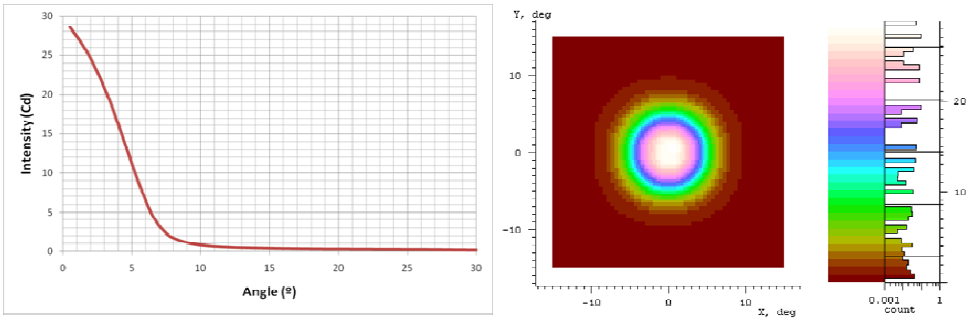

Fig. 8. Far field pattern for TIR RXI obtained in LightTools.

In order to compare the TIR RXI prototype with a conventional RIXR design, we have done the same LightTools simulation (using the same ray set of XP-G Cree LED) for a RIXR designed as explained in Section 3.1. This design has the same front and entrance surface as the TIR RXI prototype, while the back surface is smooth and metalized. Figure 9 shows the simulated far field pattern (LED power is again 1*lm*) in this case. The central lens has not been considered (we have defined it as an absorber) in this simulation. The full-width half-maximum angle is about 4° and the maximum value of the simulated intensity is 36cd/lm (this value is even higher, since there is some power lost at the central lens, which is now an absorber).

The collimation achieved with the TIR RXI is worse than in the case of the RIXR collimator. This disadvantage happens due to an approximate form of the V-grooves (there are approximated with a 90° V corners to ease the manufacturing process, see Fig. 6).

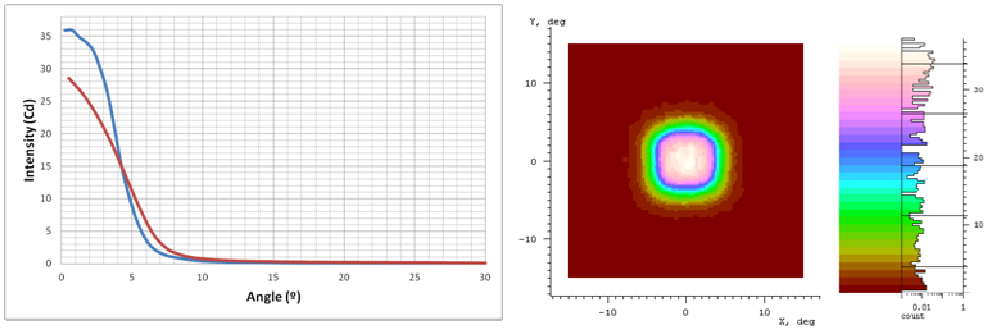

(a) (b)

Fig. 9. (a) Intensity distributions for two designs, the TIR RXI (in red) and the RIXR (in blue). (b) 2D Far field pattern for the RIXR design.

4. Colour mixing

It is well known that conventional RXI designs form an image of the source at the far field [2,3]. This feature is not good for colour mixing applications related to illumination. When four different colour LED chips are used (e.g. RGB LED) we will have four separated images of each chip at the far field. The TIR RXI makes a good colour mixing as a result of the property of the double TIR reflection on the grooved back surface, which reverses the skewness of the rays. This gives rise to a rotational smear of the far field pattern. The far field

#154985 - $15.00 USD Received 19 Sep 2011; revised 8 Nov 2011; accepted 18 Nov 2011; published 6 Dec 2011

pattern coming from an off-axis point source has ring-like shape. This effect is explained in [7,8].

Colour mixing features of both designs (with and without grooves) are simulated in LightTools. Four LEDs are modeled as perfect Lambertian sources emitting at different wavelengths. We put two green LEDs, one blue and one red LED (Fig. 10). The spacial distribution of these LEDs, their size, and optical properties are similar to a conventional RGGB white LED.

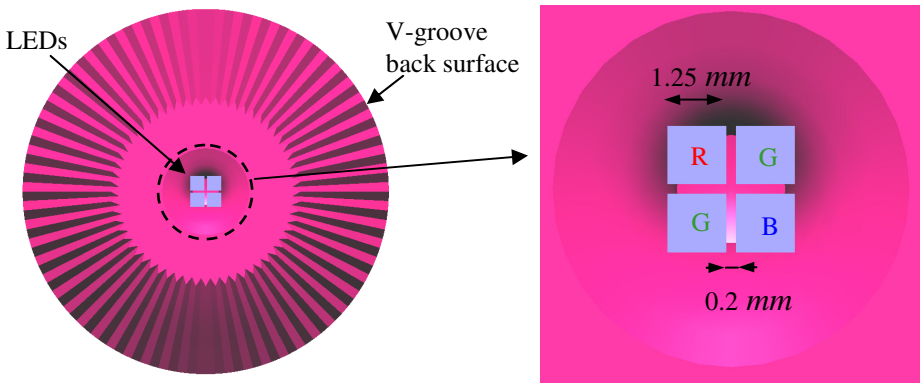

Fig. 10. Set up for LightTools colour mixing simulation.

Figure 11 shows the simulated true colour far field pattern for the metalized RIXR. The colours are not mixed, and four images of each chip can be perceived. Figure 11(b)) shows the true colour far field for the metal-less RXI collimator. Instead of the source image, we have obtained a much better colour mixing, although color separation is still visible enough to make it unacceptable for most applications.

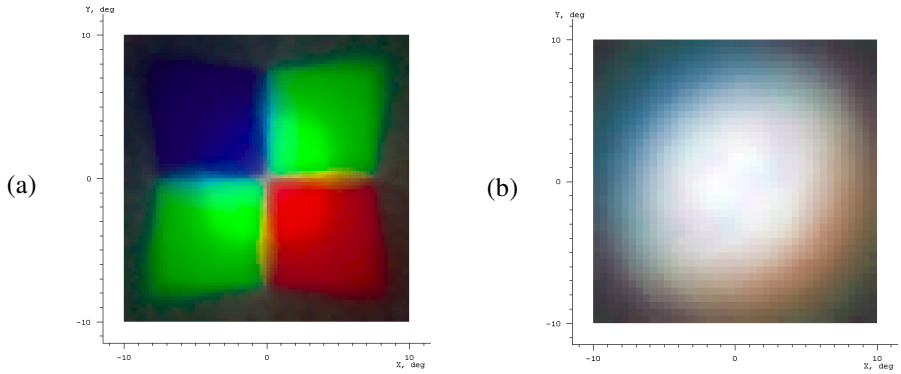

Fig. 11. Colour mixing, real colour far field patterns a) RIXR b) metal-less TIR RXI collimator.

Comparing the conventional RIXR, the TIR RXI is less sensitive to the source non-uniformities. Since the conventional RIXR provides a good source image, any source error will affect the far field pattern. As an example, we have put 4 equal cool white LEDs positioned as RGGB LED chips as detailed in Fig. 10.

#154985 - $15.00 USD Received 19 Sep 2011; revised 8 Nov 2011; accepted 18 Nov 2011; published 6 Dec 2011

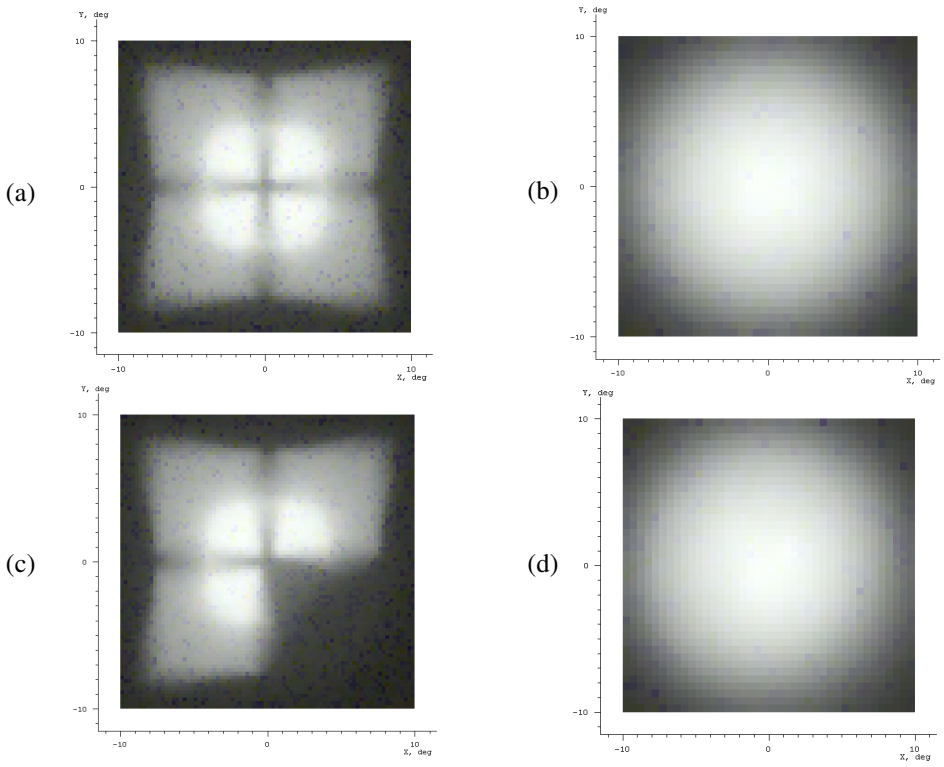

Fig. 12. LightTools real colour far field patterns (a) RIXR with four cool white LEDs, (b) TIR RXI with four cool white LEDs, (c) RIXR when one LED is turned off, (d) TIR RXI when one LED is turned off.

The RIXR forms the source image at the far field, while the TIR RXI mixes the light coming from all LED chips (Fig. 12(b)). When the conventional RIXR is used, if one of the LED chips is turned off, the form of the far field changes dramatically. Figure 12(c) shows the far field pattern simulated in LightTools (one of the LEDs is switched off). The same simulation is made for the TIR RXI (Fig. 12(d)). The form of the far field pattern remains the same as in Fig. 12(b), being only less bright as a result of the drop in the input flux.

Figure 13 shows two on axis intensity distributions individually normalized to the maximum value. The first one (the curve in blue) corresponds to the case presented in Fig. 12(b), and the second on (the curve in red) corresponds to the case presented in Fig. 12(d). From these intensity distributions, we have calculated that the maximum absolute difference in between the two patterns is 0.046, which means that the TIR RXI is very insensitive to the source non-uniformities. This allows not only the design to be made robust to chip failures, but also to provide an easy dimming strategy

#154985 - $15.00 USD Received 19 Sep 2011; revised 8 Nov 2011; accepted 18 Nov 2011; published 6 Dec 2011

Fig. 13. On axis intensity distributions normalized to the maximum value for the TIR RXI with four cool white LEDs. All the LEDs are turned on (the curve in blue). One of the LEDs is turned off (the curve in red).

5. Experimental results of the first prototype

In order to analyze the potential of the TIR RXI collimators a prototype was manufactured. Figure 14 shows the first TIR RXI prototype, made of PMMA using direct cutting with diamond turning. The geometrical measurements of the prototype have demonstrated the good quality of the cutting process. This means that the surface roughness is low and that the curvature radius of the groove peaks are small. The edges have been examined under a microscope and it has been seen that the edge curvatures fluctuations are less fluctuates being smaller than 10 μm, which is the tolerance established by the manufacturer.

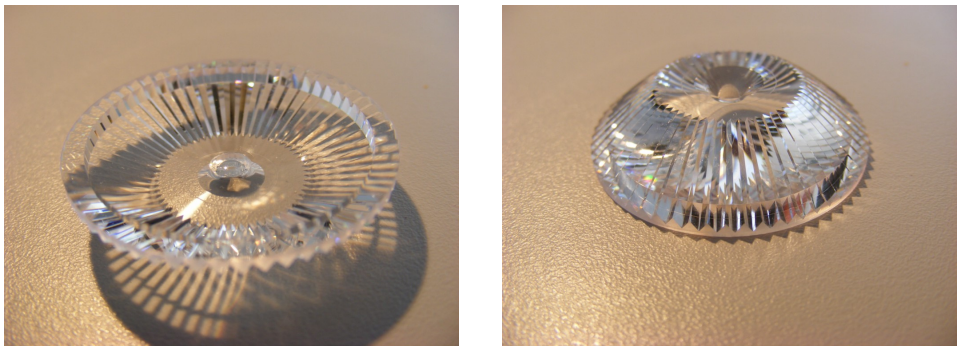

Fig. 14. Metal-less TIR RXI collimator. Manufactured prototype.

For the measurement, the TIR RXI and a XP-G Cree LED are fixed on a supportive structure. Figure 15 shows front view of the set up. In the picture on the right side, the LED was switched off, while in the picture on the left it was switched on. The grooved surface is shiny, since the rays are reflected onto it.

#154985 - $15.00 USD Received 19 Sep 2011; revised 8 Nov 2011; accepted 18 Nov 2011; published 6 Dec 2011

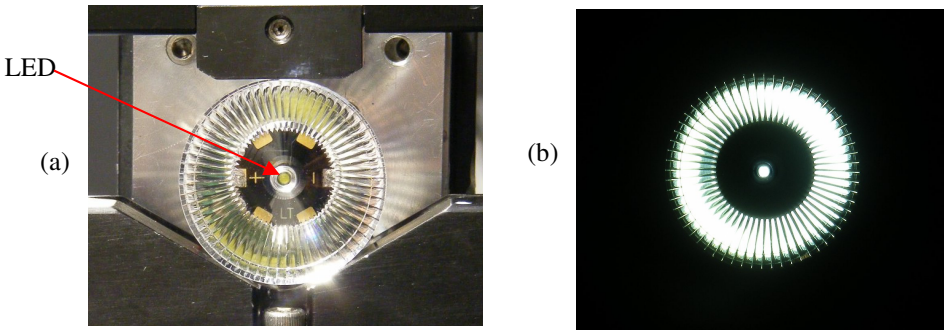

Fig. 15. Fixture of the TIR RXI collimator and the LEd. a) The LED is off, b) The LED is on.

We have captured two far field images with a calibrated camera, first, the one of the TIR RXI, and then, the one of the LED (without the collimator). According to these measurements, 70.1% of the input power reaches the far field within the rectangular ±15° (the design window, ±30°, was not measured because of the limitations in the equipment). This is very good result, since it is about 94% of the theoretical case (the LightTools simulation gives 74.9% in the same rectangle). Figure 16 shows the measured intensity distribution (for the input power of 1 *lm*). Comparing this distribution with the simulated one (Fig. 8), one can see that both graphs are very similar, with the same value of the full-width half-maximum angle of about 4.5°. The maximum value of the measured intensity 22 cd/*lm* is slightly lower than the simulated one (28cd/*lm*), probably due to scattering and the reflection on the corners of the groove.

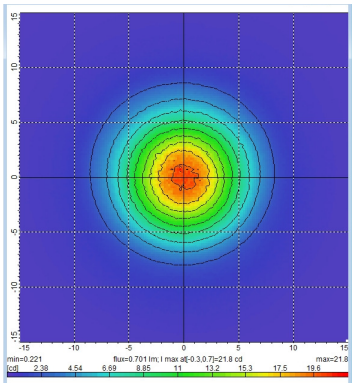

Fig. 16. Experimentally measured far field intensity distribution (for the input power of 1 *lm*).

6. Conclusions

A TIR RXI design with 60 flat V-grooves is designed, manufactured, and characterized. One of its sides is a properly calculated grooved surface that reflects the rays by means of two TIR reflections, acting as a mirrored surface in the conventional RXI. The measurements of the manufactured piece show good efficiency (about 94% of the theoretical value). The form and the shape of the measured and simulated far field patterns also coincide. This means that the first prototype has been manufactured with high accuracy. The maximum value of the measured intensity 22 cd/lum slightly differs from the simulated one (28 cd/lum). However, both have the same value of the full-width half-maximum angle (4.5°). Since the presented design does not need any metalization, the manufacturing cost is lower than in the case of the

#154985 - $15.00 USD Received 19 Sep 2011; revised 8 Nov 2011; accepted 18 Nov 2011; published 6 Dec 2011

conventional RXI. Finally, the TIR RXI performs good colour mixing as well as being very insensitive to source non-uniformities.

Acknowledgments

Authors thank the Spanish Ministries MCINN (ENGINEERING METAMATERIALS: CSD2008-00066, DEFFIO: TEC2008-03773, SIGMASOLES: PSS-440000-2009-30), MITYC (ECOLUX: TSI-020100-2010-1131, SEM: TSI-020302-2010-65), the Madrid Regional Government (SPIR: 50/2010O.23/12/09,TIC2010 and O-PRO: PIE/209/2010) and UPM (Q090935C59) for the support given in the preparation of the paper. The authors thank Synopsys (formerly Optical Research Associates) for granting us the LightTools university license.

#154985 - $15.00 USD Received 19 Sep 2011; revised 8 Nov 2011; accepted 18 Nov 2011; published 6 Dec 2011